Archives of Waste Management and Environmental Protection
Archiwum Gospodarki Odpadami i Ochrony Środowiska
ISSN 1733-4381, vol. 15, issue 3 (2013), p. 89-96
http://awmep.org

N_2O decomposition using modern micro-mesoporous materials with zeolitic properties

Małgorzata RUTKOWSKA[1], Lucjan CHMIELARZ [2], Daniel MACINA[3], Barbara DUDEK[4]

[1,2,3,4] *Faculty of Chemistry, Jagiellonian University, Ingardena 3, 30-060 Kraków, Poland tel. 126632096[1], fax. 126340515, rutkowsm@chemia.uj.edu.pl*

Abstract

In the presented studies two modern approaches of synthesis of hierarchical micro-mesoporous materials with zeolitic properties are shown. In the first synthesis the protozeolitic particles were aggregated (under specified conditions) with simultaneous creation of mesopores between the zeolite seeds. In the second synthesis the zeolite nanoseeds were impregnated on the surface of mesoporous, amorphous SBA-15 material. Both used synthesis routs resulted in formation of combined micro-mesoporous materials with zeolitic properties, what was proven by nitrogen sorption, XRD, TGA and IR-DRIFT measurements. The combination of zeolitic properties with mesopores (preferable diffusion rate) increased the accessibility of ion-exchange positions allowing the introduction of iron species nearly exclusively in the form of isolated cations. The prepared micro-mesoporous materials were tested as catalysts in low-temperature N_2O decomposition in the presence of oxygen.

Keywords: Beta zeolite, micro-mesoporous materials, ion-exchange, N_2O decomposition

Streszczenie

Rozkład N_2O przy użyciu nowoczesnych mikro-mezoporowatych materiałów o właściwościach zeolitów

W niniejszej pracy przedstawiono syntezę hierarchicznych materiałów mikro-mezoporowatych o właściwościach zeolitu, przy użyciu dwóch nowoczesnych metod. W pierwszej z nich protozeolityczne nanozarodki ulegały agregacji w odpowiednich warunkach z utworzeniem mezoporowatych przestrzeni. Druga metoda syntezy polegała na impregnacji mezoporowatego materiału SBA-15 nanoziarnami zeolitu. W przypadku obu zastosowanych metod otrzymano materiały mikro-mezoporowate o właściwościach zeolitu, co zostało potwierdzone za pomocą takich metod jak niskotemperaturowa sorpcja azotu, XRD, TGA, oraz spektroskopia IR-DRIFT. Połączenie zalet mikroporowatych zeolitów z amorficznymi materiałami mezoporowatymi zwiększyło dostępność pozycji jonowymiennych w otrzymanych materiałach. Dzięki czemu do materiałów mikro-mezoporowatych wprowadzono żelazo praktycznie wyłącznie w formie oktaedrycznie skoordynowanych kationów Fe^{3+}. Otrzymane materiały hierarchiczne zostały przebadane w roli katalizatorów niskotemperaturowego rozkładu N_2O w obecności tlenu.

Słowa kluczowe: zeolit Beta, materiały mikro-mezoporowate, wymiana jonowa, rozkład N_2O

1. Introduction

Nitrous oxide (N_2O) is one of the most dangerous air pollutants. The half-life of N_2O in the atmosphere is estimated to be between 110-170 years. Nitrous oxide intensifies the greenhouse effect (its global warming potential is about 300 times as high as that of CO_2), and the products of its decomposition in the stratosphere deplete the ozone layer. Emission of this oxide increases each year, which is mainly caused by human activities. Nowadays, the most promising way for the limitation of N_2O emissions is its catalytic decomposition to nitrogen and oxygen [1-3].

Zeolites are a very well known group of materials and have a large impact on science, technology and industrial processes. At present about 200 types of zeolites have been recognized but only less than 20 are used in industry. Thus the consideration of the modification opportunities and possibilities is a wide and open topic in this field of science. The recent progress in designed synthesis shows the trend to develop new structures with controlled

morphology, location of acid centers and crystal sizes. Combined materials with micro-and mesoporosity, so-called hierarchical materials, have been designed to overcome the diffusion limitation caused by the presence of small channels in zeolites, but also to increase the accessibility of acid centers present inside of the zeolite pore system. Both of the mentioned factors contribute to the improvement of the properties of mesoporous zeolites in comparison to conventional microporous aluminosilicates [4-6].

The presented studies were focused on synthesis of micro-mesoporous materials with zeolitic properties. Two different synthesis routes were used. Both syntheses started with the preparation of zeolite nanoparticles, which were in the first synthesis (impregnation method) impregnated on the mesoporous amorphous SBA-15 material and in the second synthesis (non-templating method) aggregated with generation of mesopores between the zeolite seeds [7, 8].

2. Catalysts preparation

The protozeolitic seeds were obtained by stopping of the zeolite Beta aging process in autoclaves at 423 K after 24 h (SiO_2: 0.02 Al_2O_3: 0.61 TEAOH: 0.20 HCl: 21 H_2O). Then the zeolite seeds suspension was used for the preparation of two series of the samples.

In the first series of the samples (non-templating method, Fig. 2.1) the zeolite seeds were acidified using HCl (18 mL of the zeolite seeds was added to 5 mL of the concentrated HCl under vigorous stirring), followed by hydrothermal treatment (72 h, 423 K). After quenching of the autoclave the sample (β-meso) was filtered, washed, dried and calcined at 823 K for 6 h.

The second series of the samples (impregnation method, Fig. 2.2) was obtained by impregnation of the zeolite seeds on the surface of SBA-15 mesoporous silica (recipe presented in [9]). Wet impregnation was used and the seeds suspensions were additionally acidified (β-SBA-15-A) or not (β-SBA-15). The impregnated samples were dried and calcined at 823 K for 6 h.

In the next step the H-forms of the micro-mesoporous samples and the reference Beta zeolite and mesoporous SBA-15 materials (β, SBA) were modified with iron by classical ion exchange method using 0.06 M solution of $FeSO_4 \cdot 7H_2O$.

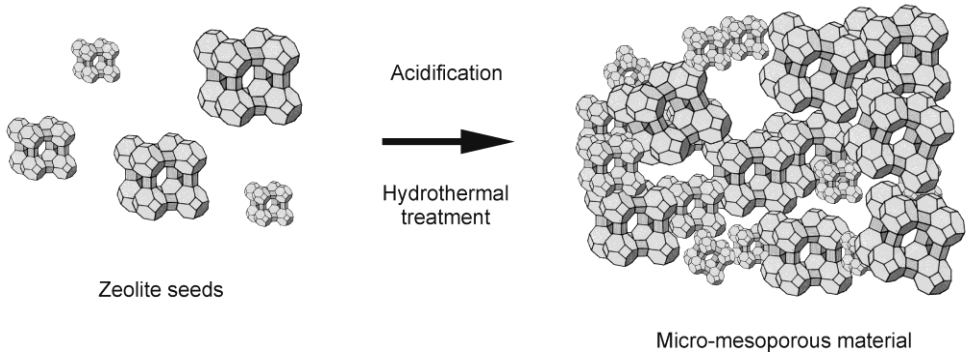

Fig. 2.1. The schema of the first path of micro-mesoporous materials synthesis (non-templating method)

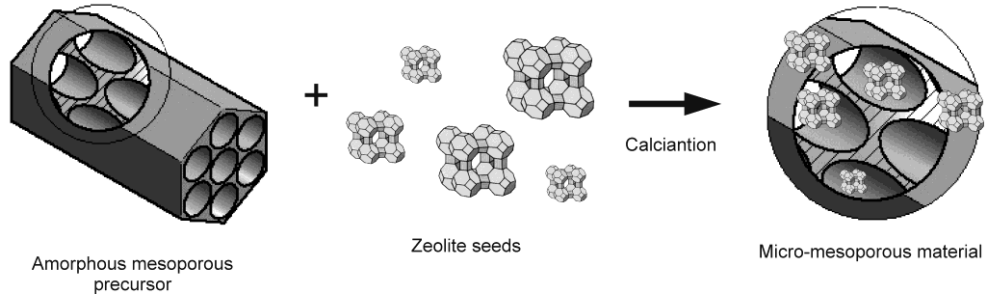

Fig. 2.2. The schema of the second path of micro-mesoporous materials synthesis (impregnation method)

3. Catalytic tests

The catalytic activity of the prepared micro-mesoporous materials (Fe-β-meso, Fe-β-SBA-15, Fe-β-SBA-15-A) and the reference samples (Fe-β, Fe-SBA-15) was examined using a gas chromatograph (SRI 8610C) equipped with TCD detector. The experiments were performed in a fixed-bed quartz microreactor using 0.1 g of catalyst (particles sizes in the range of 0.160-0.315 mm). The N_2O conversion was measured in the range of temperatures 423-823 K in intervals of 50 K. Before each measurement the sample was outgased in the flow of pure helium at 823 K, and after cooling down the mixture containing 5000 ppm of N_2O and 45000 ppm of O_2 in He (total flow 50 ml/min) was passing over the catalyst bed (measurements were done 20 min. after temperature stabilization, in a steady state conditions).

4. Results and discussion

The textural parameters of the prepared micro-mesoporous materials (β-meso, β-SBA-15, β-SBA-15-A) and the reference samples (β, SBA-15) were analyzed by low temperature nitrogen sorption measurements (ASAP 2010 Micromeritics). Table 4.1 gives an overview of the textural properties such as surface area and micropore and mesopore volumes. β-meso sample posses higher mesopore volume in comparison to conventional β sample, proving the generation of mesopores inside of the material. Lower surface area and micropore volume of this sample can be explained by shorter crystallization time. In the second series of the samples through the impregnation of SBA-15 with Beta nanoseeds the surface area and mesopore volume decreased, which indicates that the some part of the seeds was deposited at the entrance of the mesopore channels. Increase in micropore volume in the impregnated samples came from the presence of additional microporous zeolitic phase.

Table 4.1. Textural properties of the micro-mesoporous and reference samples

Sample	SBET [m^2/g]	VMIC [cm^3/g]	VMES [cm^3/g]
β	546	0.238	0.158
β-meso	519	0.135	0.752
SBA-15	809	0.118	0.949
β-SBA-15	579	0.146	0.417
β-SBA-15-A	586	0.154	0.347

The nitrogen adsorption-desorption isotherms of the prepared micro-mesoporous materials (β-meso, β-SBA-15, β-SBA-15-A) and the reference samples (β, SBA-15) are shown in Fig. 4.1. For the reference β sample the type I isotherm (according to the IUPAC classification) characteristic of microporous materials was obtained. The isotherm of the mesoporous sample prepared by the non-templating method (β-meso) posses smaller increase in the adsorbed volume of nitrogen in the range of low partial pressures in comparison to β sample. The hysteresis loop (type H3) in the range of higher nitrogen partial pressures indicated the presence of mesopores in the β-meso sample.

The nitrogen adsorption-desorption isotherms recorded for the impregnated samples and the reference SBA-15 material (β-SBA-15, β-SBA-15-A, SBA-15) possess the type IV isotherm (according to the IUPAC classification), characteristic of mesoporous materials. The hysteresis loop (of H1 type for SBA-15) was modified by impregnation to H2 type (ink bottle like pores) confirming that the zeolite Beta seeds partially blocked the mesopores channels.

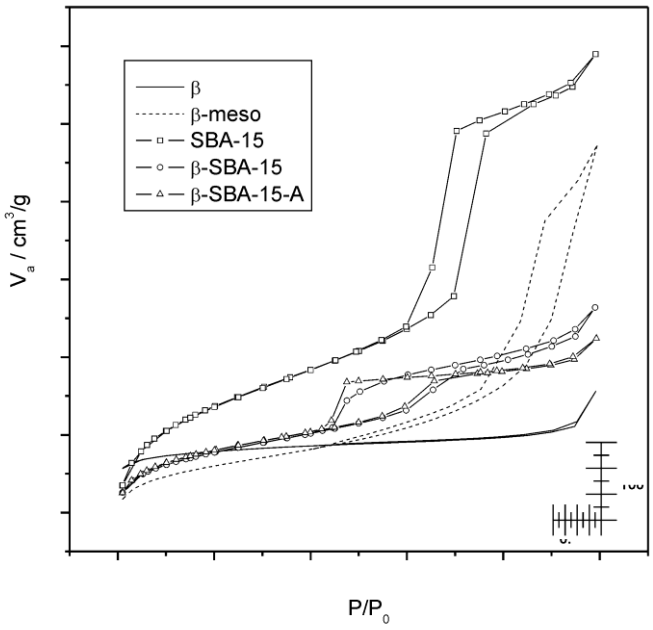

Fig. 4.1. Nitrogen adsorption-desorption isotherms of the micro-mesoporous and reference samples

The X-ray patterns (recorded using Bruker D2 Phaser instrument) of the prepared micro-mesoporous materials (β-meso, β-SBA-15, β-SBA-15-A) and the reference β sample are presented in Fig. 4.2.

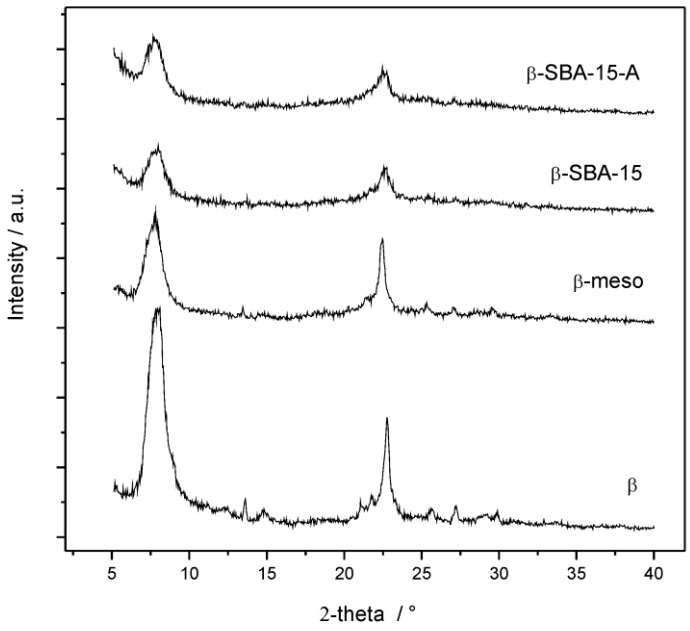

Fig. 4.2. XRD patterns of the micro-mesoporous and reference β sample

For all the micro-mesoporous samples the reflections characteristic of Beta zeolite at 2θ about 6.5-8.5° 20-25° where found. The intensity of these reflections was lower in comparison to conventional β zeolite due to the lower content of zeolitic phase (especially in case of impregnated samples).

The TGA and IR-DRIFT techniques were used to investigate the presence of zeolite Beta phase content in the obtained micro-mesoporous samples. The results (not shown) were in an agreement with the statement based on XRD patterns saying that the crystalline phase of Beta zeolite was present in the all micro-mesoporous samples.

The UV-vis-DR spectra (Evolution 600 (Thermo) spectrophotometer) of the prepared micro-mesoporous materials (Fe-β-meso, Fe-β-SBA-15, Fe-β-SBA-15-A) and the reference samples (Fe-β, Fe-SBA-15) are shown in Fig. 4.3. In case of micro-mesoporous samples iron was introduced mainly in the form of octahedrally coordinated, isolated Fe^{3+} cations (200-300 nm) and some part in the form of oligonuclear clusters (300-400 nm). The generation of mesopores between the zeolitic units enlarged the accessibility of the ion-exchange positions therefore the greater amount of iron was introduced in comparison to conventional Beta zeolite. Aditionally in case of micro-mesoporous samples the amount of bulk Fe_2O_3 aggregates (inactive in N_2O decomposition) was negligible. It is worth to mention that in case of β sample the contribution of Fe_2O_3 species is significant (probably due to the small micropores, the penetration of the zeolite channels was hindered). In case of Fe-SBA-15 only small amount of iron was introduced, due to the lack of ion-exchange properties of this material.

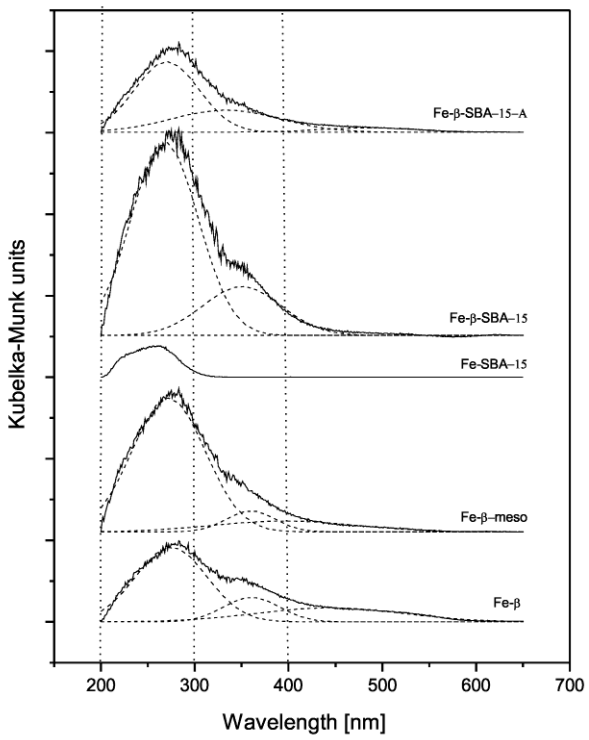

Fig. 4.3. UV-vis-DR spectra of the micro-mesoporous and reference samples

The chosen results of catalytic N_2O decomposition (at 723 and 773 K) over the prepared micro-mesoporous materials (Fe-β-meso, Fe-β-SBA-15, Fe-β-SBA-15-A) and the reference samples (Fe-β, Fe-SBA-15) are shown in Fig. 4.4.

The N_2O conversion was determined according to Equation 4.1, where c^0_{N2O} and c_{N2O} are the N_2O concentrations at the reactor inlet and outlet respectively. The calculations were performed with the assumption that for low N_2O concentration the total volumetric flow along the reactor could be considered as constant. The average from four N_2O concentrations measured in a steady state by GC was used for the calculation of nitrous oxide conversion.

$$X_{N_2O} = \frac{c^0 N_2O \ - c\, N_2O}{c^0 N_2O} \cdot 100\% \qquad \text{Eq. 4.1.}$$

The modification of mesoporous SBA-15 material with Beta nanoseeds resulted in significant increase of the catalytic activity. The most active samples Fe- β and Fe-β-meso achieved 100% of conversion at 773 K. It is worth to mention that the catalytic activity of the micro-mesoporous samples despite significantly lower content of the zeolitic phase is close to the activity of conventional Beta zeolite.

The reaction rate was calculated per 1 m^2 of the catalysts surface, according to Equation 4.2, where $\dot{n}_{N_2O}$ - is a molar flow of N_2O [mol·h^{-1}], m - catalyst weight [kg], S_{BET} - BET specific surface area [$m^2 \cdot kg^{-1}$] , X – N_2O conversion [-]. The reaction rates at 723 and 773 K, for the prepared micro-mesoporous materials (Fe-β-meso, Fe-β-SBA-15, Fe-β-SBA-15-A) and the reference Fe-β sample are shown in Table 4.2. The values obtained for the most active Fe- β and Fe-β-meso samples are similar. At 723 K the observed reaction rate for the conventional iron-exchanged Beta zeolite is slightly higher, but at 773 K the observed reaction rate is higher for the micro-mesoporous sample. The reaction rate value shows the catalyst ability to decomposition of N_2O during specified time on 1 m^2 of the surface. The decrease of the values for the impregnated samples is probably connected with smaller content of the zeolitic phase, which is a source of catalytic activity in the examined micro-mesoporous systems.

$$r = \frac{\dot{n}_{N_2O}}{m \cdot S_{BET}} \cdot X_{N_2O} \qquad \text{Eq. 4.2.}$$

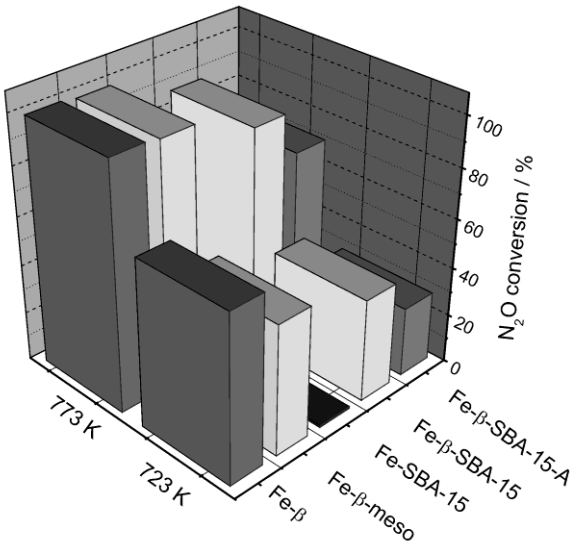

Fig. 4.4. Results of catalytic N_2O decomposition over the micro-mesoporous and reference samples

Table 4.2. Observed reaction rate at 723 and 773 K for the micro-mesoporous and reference β sample

Sample	$r_{obs.}$(723 K) [$mol \cdot m^{-2} \cdot h^{-1}$]	$r_{obs.}$(773 K) [$mol \cdot m^{-2} \cdot h^{-1}$]
Fe-β	1.4^{-7}	2.0^{-7}
Fe-β-meso	1.1^{-7}	2.1^{-7}
Fe-β-SBA-15	8.1^{-8}	1.7^{-7}
Fe-β-SBA-15-A	5.4^{-8}	1.3^{-7}

3. Conclusions

The undertaken research resulted in successful synthesis of micro-mesoporous materials. Both applied synthesis methods (impregnation and non-templating) lead to hierarchical materials with properties of Beta zeolite. The generation of mesoporosity between the zeolite units enlarged the accessibility of ion-exchange positions inside of the zeolite lattice, therefore higher amount of iron was introduced to micro-mesoporous samples. Additionally the form of iron in the hierarchical samples (octahedrally coordinated Fe^{3+} and oligonuclear clusters) is preferred for the N_2O decomposition reaction.

All the obtained micro-mesoporus samples were tested as catalyst for low temperature N_2O decomposition. The most active sample Fe-β-meso achieved 100% conversion of N_2O at 773 K. The activity of this sample is similar to the activity of the conventional Fe-β catalyst, but it should be noted that the content of zeolitic phase in hierarchical sample is much lower. The generation of mesopores had a positive effect on the catalytic activity in N_2O decomposition, simultaneously reducing the costs of catalyst preparation.

Acknowledgements

Project operated within the Foundation for Polish Science MPD Programme co-financed by the EU European Regional Development Fund.

References

1. W.C. Trogler, Coord. Chem. Rev. 187 (1999) 303-327
2. J. Pérez-Ramiréz, F. Kapteijn, K. Schöffel, J.A. Moulijn, Appl. Catal. B 44 (2003) 117-151
3. F. Kapteijn, J. Rodriguez-Mirasol, J.A. Moulijn, Appl. Catal. B 9 (1996) 25-64
4. K. Egeblad, Ch. H. Christensen, M. Kustova, C. H. Christensen, Chem. Mater. 2008, 20, 946-960
5. J. Ĉejka, S. Mintova, Cataly. Rev. 49(2007)457-509
6. A. Corma, Chem. Rev. 97 (1997) 2373-2419
7. C.J. Van Oers, W.J.J. Stevens, E. Bruijn, M.Mertens, O.I. Lebedev, G. Van Tendeloo, V. Meynen, P. Cool, Micropor. Mesopor. Mat. 120 (2009) 29-34
8. V. Meyen, P. Cool, E.F. Vansant, Micropor. Mesopor. Mat. 125 (2009) 170-223
9. V. Meynen, P. Cool, E.F. Vansant, P. Kortunov, F. Grinberg, J. Kärger, M. Mertens, O.I. Lebedev, G. Van Tendeloo, Micropor. Mesopor. Mat. 99 (2007) 14-22